Desalination and Water Treatment
www.deswater.com

doi: 10.5004/dwt.2023.29820

304 (2023) 210–218
August

Improved electrochemical recovery of metallic powder from acidic chloride-citrate electrolyte

Bingbing Li[a,*], Yi Hu[a], Mo Huang[b,*]

[a]*School of Energy and Chemical Engineering, Tianjin Renai College, Tianjin 301636, China, emails: libb03@tju.edu.cn (B. Li), huyitjrac@163.com (Y. Hu)*
[b]*Audit Department, Jiangxi University of Traditional Chinese Medicine, Nanchang 330004, China, email: huangmo90@jxutcm.edu.cn (M. Huang)*

Received 3 February 2023; Accepted 1 August 2023

ABSTRACT

Metal recovery from acidic chloride systems is significant for large-scale environmental remediation and sustainable metals recycling. However, there is a scarcity of electrodeposition processes suitable for acidic chloride media. Herein, an energy-efficient electrochemical recovery process for copper (Cu), selenium (Se), and tellurium (Te) recovery was first presented. The combination of a turbulent reactor with stainless steel electrode and an acidic chloride-citrate electrolyte led to a notable improvement in dilute metal electrodeposition recovery from the HCl system. The addition of citrate generated a synergistic improvement in metal electrodeposition from dilute solutions, effectively inhibiting unfavorable electrochemical reduction pathways. The enhanced mass transfer facilitated by the reactor further enhanced the quality, recovery, and current efficiency of the deposited metals. As a result, >98% Cu, Se, and Te were successfully extracted as a fine powder with a high current efficiency of 90%. This strategy presents an alternative, low-cost, and efficient platform for metal recovery and wastewater remediation.

Keywords: Electrochemical recovery; Hydrochloric acid; Electrodeposition; Citrate; Mass transfer-enhanced reactor; Metallic powder

1. Introduction

Recently, the metallurgical industry has been generating approximately 12 million tonnes of copper anode slimes annually [1–3]. Improper disposal of these slimes not only leads to a loss of valuable resources but also poses a significant threat to environmental pollution. It has been demonstrated that significant amounts (5 kg/ton) of valuable elements, including copper (Cu), selenium (Se), and tellurium (Te), are present in these anode slimes [4–7]. Se and Te are critical strategic metals with limited natural availability, widely used in industries such as semiconductors, electronics, and renewable energy technologies like solar panels, LEDs, and phase-change memory chips [8,9]. Notably, around 90% of Se and Te are sourced from copper anode slimes formed during electrolytic refining. Consequently, the exploration of resource recovery processes from these waste streams is of great importance to effectively utilize the metal resources and protect the global environment [10–12].

Conventional cost-effective methods for Se and Te recovery, such as chemical precipitation and solvent extraction, encompass techniques like sulfation roasting-acid leaching, oxidation roasting-alkali leaching, soda roasting-acid leaching, oxygen pressure leaching, chlorination leaching, and others [13,14]. However, these methods often encounter challenges like sludge generation and the production of low-grade products [15–17].

Alternatively, electrodeposition is a highly selective and efficient technique to extract metal ions in the most valuable metallic state [18–23]. Considerable electrodeposition

* Corresponding author.

processes have been successfully developed in acidic sulfate media, while few are available in acidic chloride media [24–27]. This is mainly due to the aggressive nature of the HCl system, in which the cathode dissolution and CuCl precipitation are severe [28,29]. Besides, the overall current efficiency is very low (<60%), and metal deposit quality is poor in this system. Recently, it has been demonstrated that citrate medium is a promising chelating agent to form various complexes with copper ions, significantly facilitating the metal electrodeposition performance [30–35]. Many copper and copper alloys have been readily electrodeposited from the additive-free citrate bath.

Besides, it is widely recognized that the mass transfer conditions significantly influence the electrodeposition process. Factors such as the use of electrode movements, high surface area cathodes, or fast solution flow rates play crucial roles in ensuring efficient electrodeposition [36–39]. Jin et al. [40] implemented a two-stage emew® cell process to enhance the extraction of bismuth and copper from a waste stream generated during copper electrorefining, resulting in remarkable recovery rates of 93.4% for bismuth and 97.8% for copper, and the overall current efficiency of the process was recorded at 62%. Barragan et al. [41] utilized a rotating cylinder electrode electrochemical reactor to enhance the purity of recovered copper and antimony metals from electronic waste, resulting in a 96 wt.% pure copper deposit and an 81 wt.% pure antimony precipitate.

Therefore, this study aims to evaluate the effect of citrate on the dilute metal (Cu, Se, and Te) electrodeposition from the HCl system. Besides, the deposits' quality, recovery, and current efficiency are also expected to be improved via the mass transfer-enhanced reactor. The significance of this research lies in its efficient metal recovery from acidic chloride systems, promoting sustainable metal recycling and wastewater remediation. The production of microscale fine particles has potential benefits in powder metallurgy and catalysis. Moreover, the insights gained from this study can be applied to other valuable metals, opening new avenues for metal recovery research and materials fabrication.

2. Experimental set-up

Analytical grade chemical reagents were received from Sigma-Aldrich (St. Louis, MO, USA), including sodium citrate dehydrate (≥99.0 wt.%), copper chloride (>99.99 wt.%), sodium selenite (>99.99 wt.%), sodium tellurite (>99.99 wt.%) and hydrochloric acid (>99.0 wt.%). The solutions were prepared by dissolving the corresponding reagents into ultrapure water (18 MΩ/cm).

To investigate the fundamental electrochemistry of Cu, Se, and Te electrodeposition, cyclic voltammetry (CV) and linear sweep voltammetry (LSV) experiments were conducted in nitrogen-purged solutions at 25°C. A CHI760E workstation (CH Instruments, Shanghai) was utilized for these electrochemical studies, following the procedure established by Jin et al. [18,37]. Electrochemical impedance spectra were measured from 200 kHz to 2 mHz with an AC voltage amplitude of 10 mV. It should be noted that the open circuit potentials of 0, 10, and 20 g/L citrate are 0.07, 0.07, and 0.13 V, respectively. A three electrodes cell (100 mL) was employed with a 1.0 cm^2 316 L stainless steel working electrode, an IrO_2-Ta_2O_5 coated Ti counter electrode, and an Ag/AgCl (0.22 V vs. SHE) reference electrode. Chronopotentiometry (CP) was employed to investigate the electrodeposition behavior with the same electrochemical cell and electrodes as described in the CV procedure. To enhance the mass transfer condition, a cylinder turbulent reactor (emew® cell) with an IrO_2-Ta_2O_5 coated Ti anode in the center and an annular 316 L stainless steel foil cathode was employed to investigate the metal electrodeposition performance. The cell possesses a 350 cm^2 cathode and 200 cm^2 anode, while the current density was set at 300 A/m^2. 2 L solution was tested with a flow rate of 3–6 L/min.

The Cu_2Se content in the experiment was estimated from the peak area of the X-ray diffraction (XRD) results, while the elemental contents (Cu, Se, and Te) are calculated based on XRD and energy-dispersive X-ray spectroscopy (EDS). The Cu(II)-citrate complexation was determined with a Labtech 9100B UV-Vis spectrophotometer. The Cl^- concentration was measured with the ion chromatograph DX-500 (Dionex, USA). The surface morphology and element composition of deposits were characterized using field-emission scanning electron microscopy (FE-SEM, JSM-7610F). The crystalline structure was examined using X-ray diffraction (XRD, Smartlab, Japan, Cu Kα radiation). The concentration of copper ions was measured with an inductivity-coupled plasma-optical emission spectrometer (ICP-OES, Optima 5300DV, PerkinElmer, USA). The powder size and distribution were collected from a Microtrac S3500 particle size analyzer after 60 min sonication.

3. Results and discussion

3.1. Copper electrodeposition

Cyclic voltammetry (CV) and linear sweep voltammetry (LSV) investigations were performed to study the electrochemical reduction of the Cu(II) in hydrochloric acid (blank) and citrate acid media. And the results are shown in Fig. 1.

As depicted in Fig. 1a, the HCl (blank) solution exhibited a conspicuous oxidation peak at –0.02 V and a very small reduction peak at –0.30 V, corresponding to the Fe^{2+}/Fe^{3+} reactions taking place at the stainless-steel electrodes [42]. In contrast, when 3 g/L (0.047 mol/L) Cu(II) was present, a distinct reduction peak was observed at –0.27 V with a peak current density of 31 mA/cm^2. Notably, no noticeable reduction peak was observed in the same potential region of the corresponding blank solution, which unequivocally suggests that this peak is attributed to Cu(II) reduction. Upon the successive addition of citrate, a notable positive shift in the Cu(II) reduction peak potential to –0.24 V was observed, accompanied by a significant increase in peak current density to 48 mA/cm^2 (as depicted in Fig. 1c). These observations indicate the facilitative effect of citrate on the reduction process, arising from both thermodynamic and kinetic considerations. Remarkably, during repeated tests, the reduction potentials and currents of copper ions are reproducible (as shown in Fig. 1b and d).

To evaluate the solution chemistry of this system, Fig. 2a shows the UV-Vis spectra for 3 g/L Cu(II) solution at different concentrations of citrate. It can be seen that the characteristic peak at 832 nm monotonically increases with the

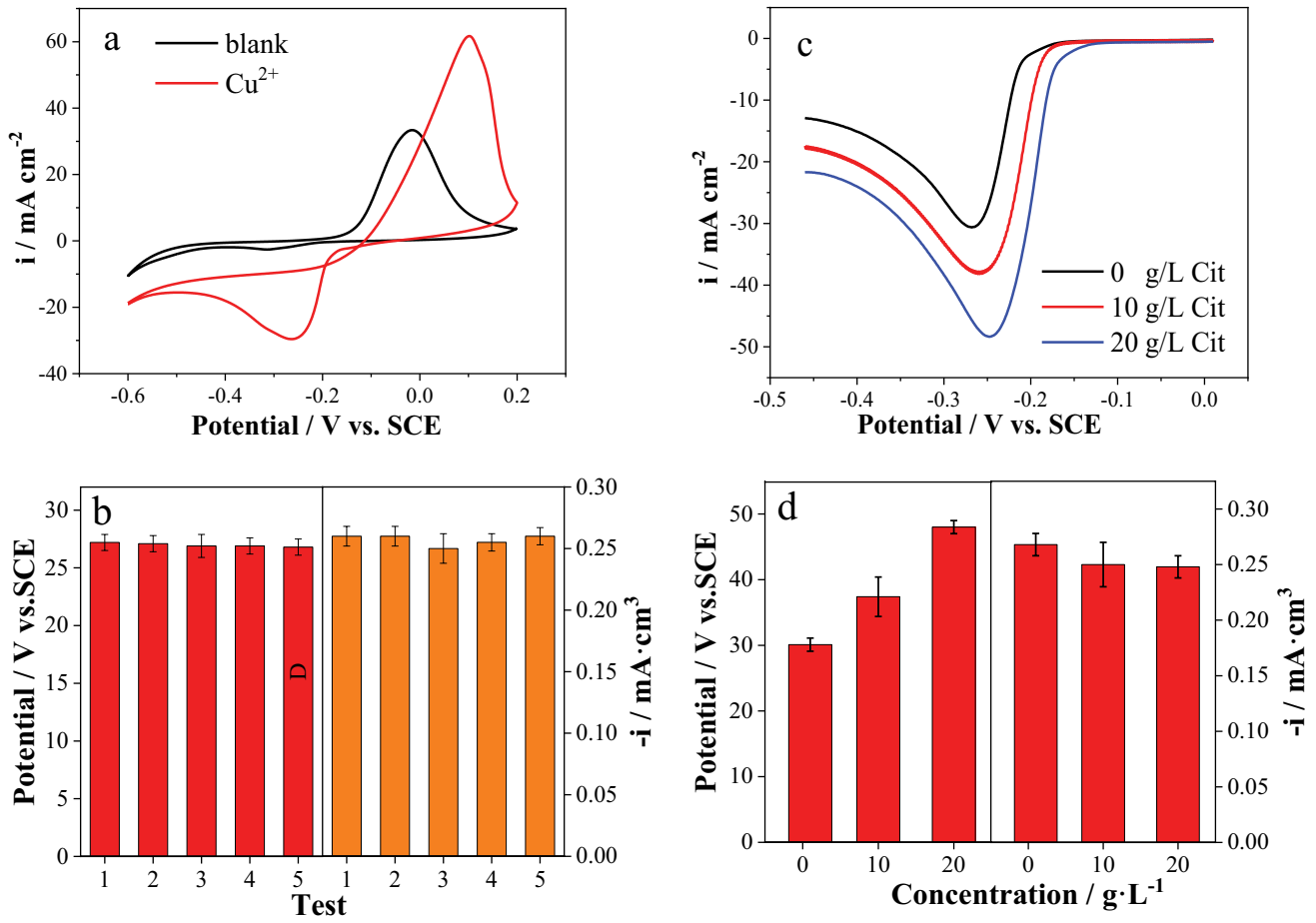

Fig. 1. (a) Cyclic voltammograms of stainless-steel electrode with and without 3 g/L Cu^{2+} in the 35 g/L HCl solutions, (b) the repeatability of the CV measurements, (c) linear sweep voltammograms of 3 g/L Cu^{2+} and 35 g/L HCl in different citrate concentrations, scan rate: 100 mV/s, and (d) the repeatability of the CV measurements at different citrate concentrations.

addition of citrate, suggesting a stronger complex association. Furthermore, a similar phenomenon was observed in the electrochemical impedance spectroscopy as shown in Fig. 2b. The Nyquist plots exhibited a semi-ellipse at a high-frequency region and an inclined line at a low-frequency region. It should be noted that Z′ axis at high frequency is related to the resistance of the electrolytes (Rs), while the semicircle in the middle-frequency range stems from the charge transfer resistance (Rct) at the electrode/electrolyte interface. It can be seen that there is no significant slope change of the linear part in the low-frequency region, suggesting good ionic diffusion. With the increasing citrate addition, the impedance semicircles of Nyquist plots increase and the resistance value increases from ~0.86 to 1.28 Ω, indicating that further complexation is achieved in the system. It has been identified that the copper reduction kinetics is closely related to the complexation chemistry, and the rate constant is frustrated with the increasing copper-citrate chelation in the citrate bath [43]. Interestingly, it is not inconsistent with the conclusion of Fig. 1a, which requires further illustration in the following sections.

To enhance the mass transfer and improve the electrochemical metal recovery from the acidic chloride-citrate systems, a cylinder turbulent electrochemical cell with a larger cathode surface area was employed for the dilute metal electrodeposition [40]. As shown in Table 1, 76% copper is recovered from the acidic chloride solution with a current efficiency of 61%. And the powder consists of Cu, Cu_2O, and CuCl as shown in Fig. 3. The specific composition of electrodeposit can be calculated to be 25% Cu_2O, 70% Cu, and 5% CuCl, indicating the involvement of incomplete electrochemical copper reduction and chloride-mediated pathways [44]. It has been demonstrated that there is chloride-mediated electrodeposition of copper ions [Eqs. (1) and (2)], as well as side reactions of chlorine evolution at the anode [Eq. (3)], which may contribute to the unsatisfactory copper recovery ratio. However, the performance is substantially improved by the successive addition of citrate.

$$Cu^{2+} + Cl^- + e^- = CuCl_{ads} \quad (1)$$

$$CuCl_{ads} = Cu + Cl^- \quad (2)$$

$$2Cl^- = Cl_2 + 2e^- \quad (3)$$

In contrast, 99% copper is successfully extracted with a higher current efficiency of 84% in the presence of 20 g/L

(0.077 mol/L) citrate, offering promising performance for potential industrial applications. Furthermore, the impurity of CuCl is entirely avoided, and only 6% Cu_2O is obtained in the product (Fig. 3 and Table 1). And the final Cl^- concentration is nearly 35 g/L, indicating the anodic chlorine evolution is also substantially inhibited. This indicated the low-efficiency chloride-mediated pathways were efficiently eliminated, and the incomplete reduction pathway was greatly inhibited due to the increasing citrate complexation. It should be noted that the current efficiency was estimated with Eq. (4) by considering the corresponding electron transfer numbers of different products [18], while the copper, selenium, and tellurium were calculated with Eq. (5) by considering the extracted copper, selenium, and tellurium from the HCl solutions:

$$\mathrm{CE} = \frac{96485\sum_{n=1}^{\infty}\frac{nm}{M}}{i \times t} \tag{4}$$

$$\eta = \frac{a \times \omega}{b} \tag{5}$$

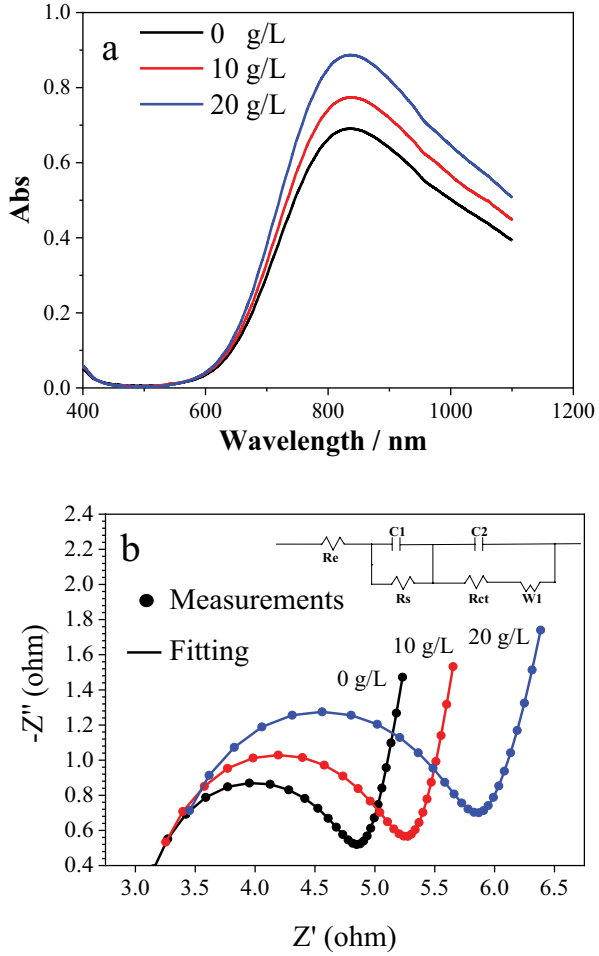

Fig. 2. (a) UV-Vis spectra and (b) electrochemical impedance spectroscopy of acidic copper chloride solution at different concentrations of citrate.

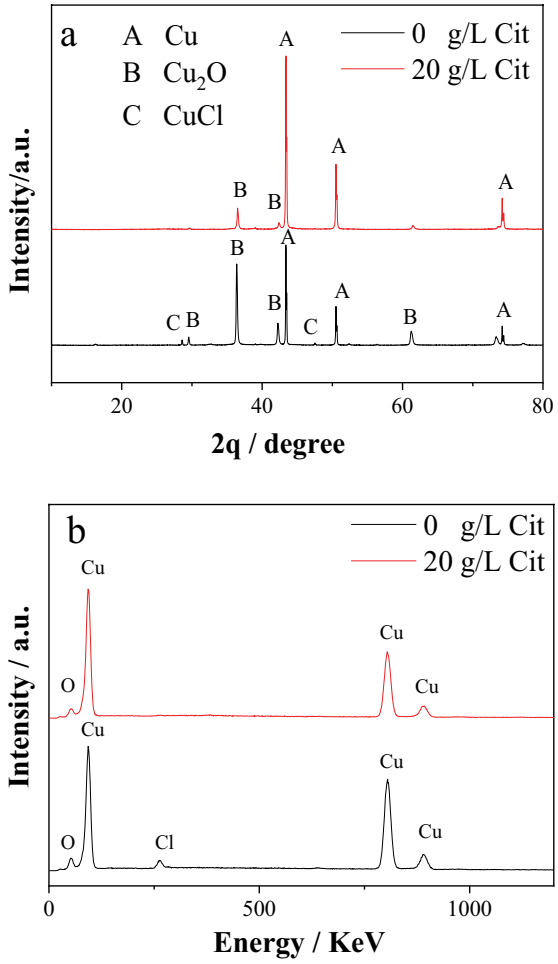

Fig. 3. Comparison of (a) X-ray diffraction and (b) energy-dispersive X-ray spectroscopy spectra of electrodeposited copper powder in the absence and presence of 20 g/L citrate.

Table 1
Comparison of electrodeposition processes with different citrate concentrations in the cylinder tubular reactor

Citrate concentration (g/L)	Mass transport (L/min)	Time (min)	Current efficiency	Cu recovery	Final Cl^- (g/L)	Product composition
0	3	40	61%	76%	32.2	25% Cu_2O, 70% Cu, 5% CuCl
10	3	40	72%	88%	32.9	15% Cu_2O, 83% Cu, 2% CuCl
20	3	40	84%	99%	34.3	6% Cu_2O, 92% Cu
10	6	40	89%	98%	34.7	3% Cu_2O, 97% Cu

in which the CE is the current efficiency, 96,485 C/mol is the Faraday constant, n is electron transfer numbers, m and M are the corresponding weight and molar mass of deposits, respectively; η is recovery ratio, a is the weight of as-prepared deposits, ω is the mass fraction of metal in the powder product, and b is the total weight of metal.

Furthermore, the increase in mass flow rate from 3 to 6 L/min, as shown in Table 1, resulted in improved recovery performance, even with a reduced amount of citrate. This enhancement further led to an increase in the purity of copper to 97%. The findings suggest that improving mass transport is also crucial for efficient metal electrodeposition from diluted solutions. The uniform fluid velocity and effective diffusion coefficient of the turbulent reactor play a pivotal role in inhibiting the formation of undesirable deposited products and side chlorine evolution reactions [37]. The optimized mass transfer condition in the turbulent reactor significantly contributes to the overall improvement in the recovery performance and purity of the electrodeposited metals.

3.2. Simultaneous electrodeposition behavior

Linear sweep voltammetry (LSV) and chronopotentiometry (CP) investigations were performed in different citrate concentrations at 350 A/m^2 to study the simultaneous electrodeposition of Cu(II), Se(IV), and Te(IV) in hydrochloric acid (blank) and citrate acid media. And the results are shown in Fig. 4.

As shown in Fig. 4a, there is a reduction peak at –0.035 V in the solution without citrate, which is due to the combination of Cu(II), Se(IV), and Te(IV) reduction peaks. However, with the continuous addition of citrate, the peak current density significantly increases to 37 mA/cm^2, and the reduction peak potential shifts negatively to –0.12 V. This shift indicates that citrate enhances the electrodeposition kinetics, leading to improved reduction of the metal ions.

Additionally, Fig. 4b demonstrates a noticeable potential negative shift, from –0.64 to –0.78 V, upon the addition of citrate at a current density of 350 A/m^2. This observation further confirms that the presence of citrate provides an increased driving force for electrochemical metal recovery. The shift towards more negative potentials indicates enhanced reduction kinetics and improved efficiency in simultaneously recovering Cu, Se, and Te ions from the acidic chloride-citrate electrolyte. Overall, these results highlight the beneficial impact of citrate in promoting the electrodeposition process and facilitating the recovery of multiple metals simultaneously.

Furthermore, electrolytic metal recovery using the cyclone electrowinning cell was examined for 50 min, and deposition products were removed and collected. Fig. 5a shows the results of the EDS analyses, indicating that the products consist of Cu, Se, and Te. Additionally, Fig. 5b, which represents XRD data, confirms the presence of Cu, Se, Te, and Cu_2Se in the obtained products. As compared to the 0 g/L citrate solution (Sample 1), the content of Cu_2Se is significantly reduced when citrate was added (Sample 2). And further improvement of copper electrodeposition is achieved as illustrated in Fig. 5a.

As shown in Table 2, when using a solution flow rate of 3 L/min, a highly efficient recovery of 99% copper, 98% selenium, and 99% tellurium was achieved from the acid solution with a concentration of 20 g/L citrate. Notably, the current efficiency in this case was determined to be 89%, which is significantly higher than the corresponding 64% achieved in the absence of citrate (0 g/L citrate solution). It can be seen that the cathodic side-reaction of hydrogen evolution is greatly frustrated. By optimizing the mass transfer conditions and increasing the solution flow rate to 6 L/min, we were able to achieve similar recovery performance for metals (Cu, Se, and Te) with a significantly lower concentration of citrate at 5 g/L. This improvement in mass transfer enhanced the electrodeposition process, allowing for more efficient metal recovery even at lower citrate concentrations. At the same time, there is a synergistic effect for the reinforced electrochemical copper deposition behavior in this chloride-citrate system.

To evaluate the metal deposit quality, the morphology and particle size of the recovered metals from the acidic chloride-citrate system using the mass transfer-enhanced reactor were evaluated, and the results are presented in Fig. 6.

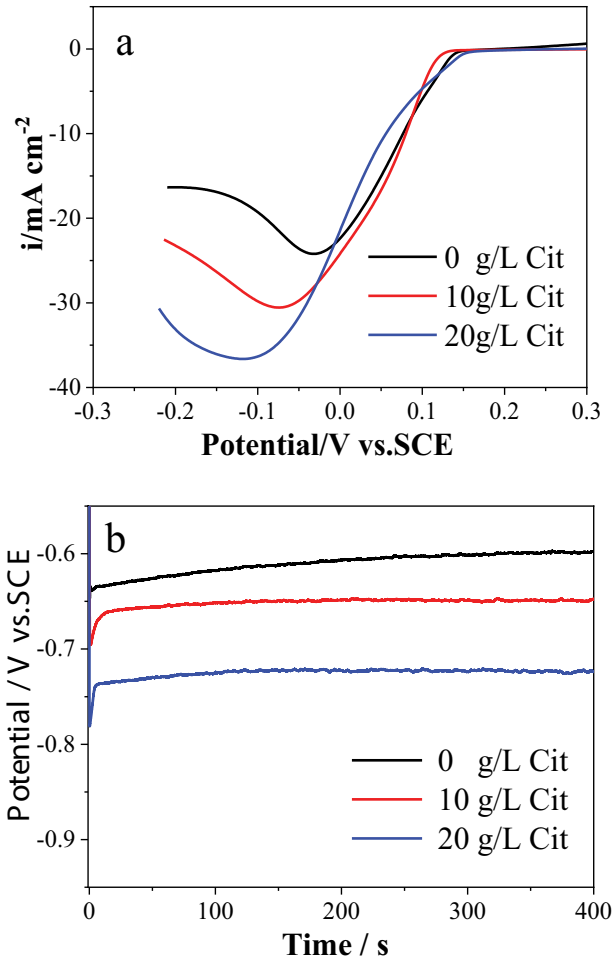

Fig. 4. (a) Linear sweep voltammetry (scan rate: 100 mV/s) and (b) chronopotentiometry curves of 1 g/L Cu^{2+}, 0.5 g/L Te^{4+}, and 0.5 g/L Se^{4+} in different citrate concentrations at 350 A/m^2.

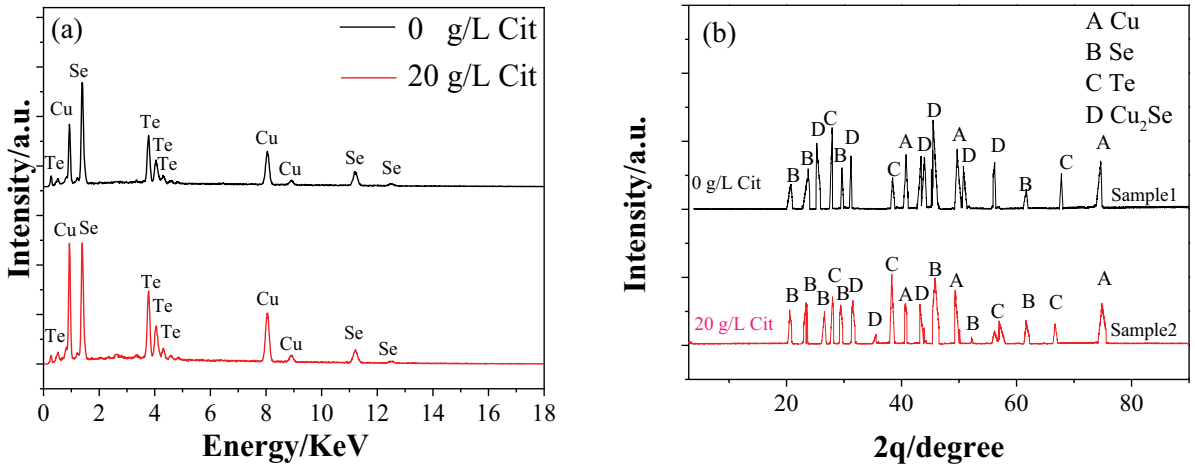

Fig. 5. (a) Energy-dispersive X-ray spectroscopy and X-ray diffraction (b) spectra of electrodeposition film from 0 and 20 g/L citrate containing 1 g/L Cu^{2+}, 0.5 g/L Se^{4+}, 0.5 g/L Te^{4+}, and 0.5 M HCl.

Table 2
Comparison of electrodeposition processes with different citrate concentrations in the cylinder tubular reactor

Citrate concentration (g/L)	Mass transport (L/min)	Time (min)	Current efficiency (%)	Cu recovery (%)	Se recovery (%)	Te recovery (%)	Products composition (wt.%)
0	3	50	64	77	78	75	%20Cu, %24Se, %36Te, %20Cu_2Se
10	3	50	73	89	90	88	%24Cu, %26Se, %35Te, %15Cu_2Se
20	3	50	89	99	98	99	%32Cu, %32Se, %31Te, %5Cu_2Se
7	5	50	88	98	97	95	%27Cu, %28Se, %31Te, %14Cu_2Se
5	6	50	90	99	98	99	%34Cu, %33Se, %29Te, %4Cu_2Se

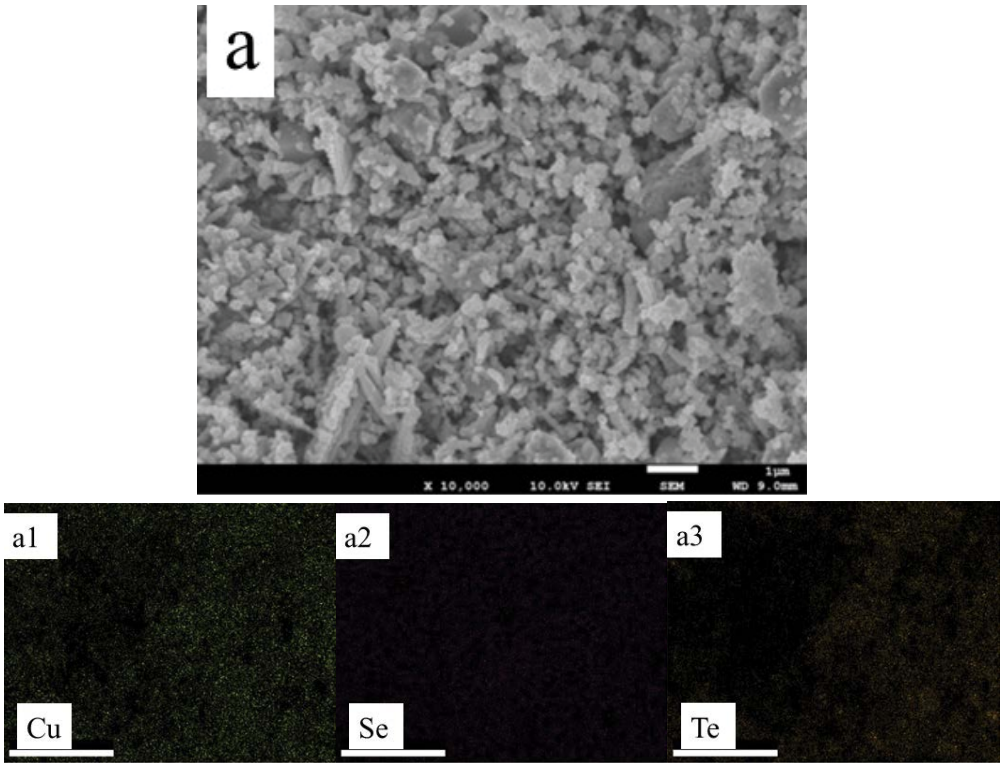

Fig. 6 (Continued)

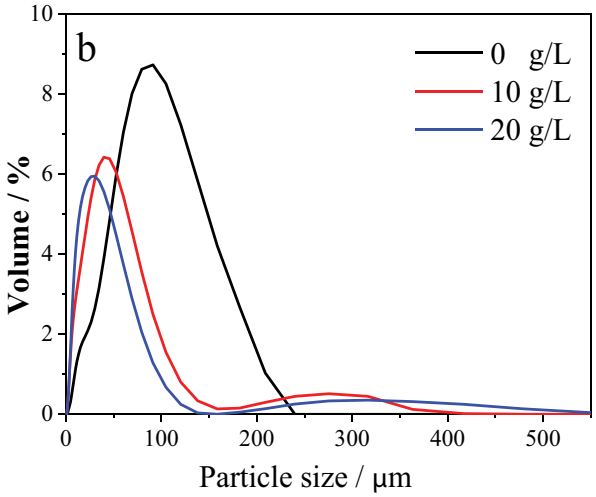

Fig. 6. (a) Scanning electron microscopy image of electrodeposited powder from acidic copper, selenium, and tellurium chloride bath in the presence of 20 g/L citrate and the mapping image of different qualities (a1, a2 and a3) and (b) particle-size distribution of deposited powders at different concentration of citrate.

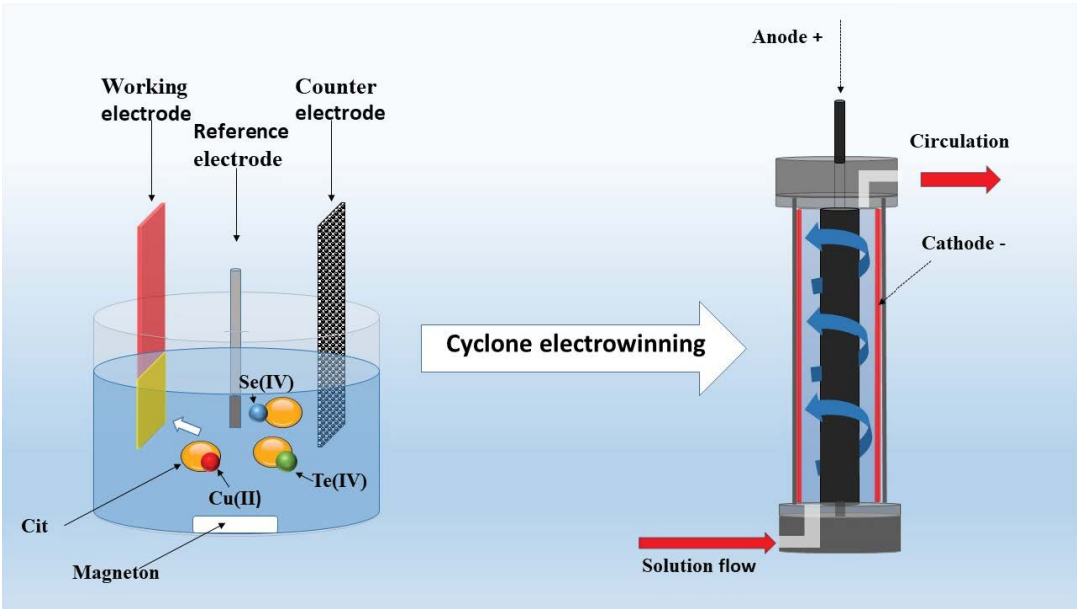

Fig. 7. Schematic diagrams of improved electrodeposition of fine copper, selenium, and tellurium particle from acidic chloride-citrate electrolyte.

The analysis revealed that the deposits exhibited a microscale fine particle morphology, and the particle-size distribution showed a decreasing trend with the addition of citrate. Indeed, the cylinder turbulent cell demonstrated a significant advantage over the conventional cell in terms of producing electrodeposited microscale fine particles. This improved performance can be attributed to the enhanced transport facilitated by cyclone electrowinning in the turbulent reactor. The efficient mass transfer and uniform fluid velocity within the turbulent cell contributed to the formation of fine particles, resulting in a more desirable and efficient electrodeposition process for copper, selenium, and tellurium.

The schematic diagrams depicted in Fig. 7 provide an insight into the enhanced electrodeposition of fine copper, selenium, and tellurium particles from the acidic chloride-citrate electrolyte. These microscale particles hold great promise in applications such as powder metallurgy and chemical catalysis, indicating the potential for efficient and sustainable materials fabrication and wastewater treatment. The success of this electrochemical recovery process represents a significant step forward in metal extraction from acidic chloride systems, contributing to large-scale environmental remediation and advancing sustainable metals recycling practices.

4. Conclusions

In summary, an efficient and selective electrochemical extraction process for dilute Cu, Se, and Te ions from an aggressive hydrochloric acid system was successfully developed by combining a tubular reactor with an acidic chloride-citrate electrolyte. Firstly, the impact of citrate on the dilute metal electrodeposition from the HCl system was examined through cyclic voltammetry and linear sweep voltammetry investigations. Remarkably, the addition of citrate demonstrated a synergistic enhancement in metal electrodeposition from dilute solutions, effectively suppressing unfavorable electrochemical reduction pathways.

Additionally, the performance of metals (Cu, Se, and Te) electrodeposition was investigated using a cylinder turbulent reactor (emew® cell) with an IrO_2-Ta_2O_5 coated Ti anode in the center and an annular 316 L stainless steel foil cathode, to optimize the mass transfer conditions. Notably, the utilization of the mass transfer-enhanced reactor in an acidic chloride-citrate electrolyte led to significant improvements in the quality, recovery, and current efficiency of the deposits. As a result, >98% copper, selenium, and tellurium were successfully extracted as fine (microscale) powder with a high current efficiency of 90%, offering a promising process for wastewater treatment and materials fabrication.

In conclusion, this study showcased an energy-efficient electrochemical recovery process for metal extraction from acidic chloride systems. The combination of a turbulent reactor and an acidic chloride-citrate electrolyte represented a significant advancement in the field of metal recovery. Moreover, the addition of citrate facilitated electrodeposition kinetics, providing a higher driving force for metal recovery and improving current efficiency. This strategy offers great potential for various industrial applications and contributes to sustainable metals recycling and environmental remediation efforts.

Conflicts of interest

There are no conflicts to declare.

Acknowledgments

We acknowledge the funding support from Tianjin Research Innovation Project for Postgraduate Students (Grant No. 2019KJ149).

Symbols

CE	—	Current efficiency
n	—	Electron transfer numbers
m	—	Corresponding weight of deposits
M	—	Corresponding molar mass of deposits
η	—	Recovery ratio
a	—	Weight of as-prepared deposits
ω	—	Mass fraction of metal in the powder product
b	—	Total weight of the metal

References

[1] Y.H. Zhang, S.L. Liu, H.H. Xie, X.L. Zeng, J.H. Li, Current status on leaching precious metals from waste printed circuit boards, Procedia Environ. Sci., 16 (2012) 560–568.
[2] H. Wang, H.L. Song, R. Yu, X. Cao, Z. Fang, X.N. Li, New process for copper migration by bioelectricity generation in soil microbial fuel cells, Environ. Sci. Pollut. Res. Int., 23 (2016) 13147–13154.
[3] V. Rai, D.B. Liu, D. Xia, Y. Jayaraman, J.-C.P. Gabriel, Electrochemical approaches for the recovery of metals from electronic waste: a critical review, Recycling, 6 (2021) 53, doi: 10.3390/recycling6030053.
[4] T. Zubala, M. Patro, P. Boguta, Variability of zinc, copper and lead contents in sludge of the municipal stormwater treatment plant, Environ. Sci. Pollut. Res. Int., 24 (2017) 17145–17152.
[5] Z.Q. Zhang, Y. Zhou, J. Zhang, S.Q. Xia, Copper(II) adsorption by the extracellular polymeric substance extracted from waste activated sludge after short-time aerobic digestion, Environ. Sci. Pollut. Res. Int., 21 (2014) 2132–2140.
[6] L.P. Wang, Y.J. Chen, Sequential precipitation of iron, copper, and zinc from wastewater for metal recovery, J. Environ. Eng., 145 (2019) 04018130, doi: 10.1061/(ASCE)EE.1943-7870.0001480.
[7] Z.L. Dong, T. Jiang, B. Xu, J.K. Yang, Y.Z. Chen, Q. Li, Y.B. Yang, Comprehensive recoveries of selenium, copper, gold, silver and lead from a copper anode slime with a clean and economical hydrometallurgical process, Chem. Eng. J., 393 (2020) 124762, doi: 10.1016/j.cej.2020.124762.
[8] G. Kavlak, T.E. Graedel, Global anthropogenic selenium cycles for 1940–2010, Resour. Conserv. Recycl., 73 (2013) 17–22.
[9] G. Kavlak, T.E. Graedel, Global anthropogenic tellurium cycles for 1940–2010, Resour. Conserv. Recycl., 76 (2013) 21–26.
[10] U. Jadhav, H. Hocheng, Hydrometallurgical recovery of metals from large printed circuit board pieces, Sci. Rep., 5 (2015) 14574, doi: 10.1038/srep14574.
[11] S. Hedrich, R. Kermer, T. Aubel, M. Martin, A. Schippers, D.B. Johnson, E. Janneck, Implementation of biological and chemical techniques to recover metals from copper-rich leach solutions, Hydrometallurgy, 179 (2018) 274–281.
[12] M.Q. Li, N. Chen, H. Shang, C.C. Ling, K. Wei, S.X. Zhao, B. Zhou, F.L. Jia, Z.H. Ai, L.Z. Zhang, An electrochemical strategy for simultaneous heavy metal complexes wastewater treatment and resource recovery, Environ. Sci. Technol., 56 (2022) 10945–10953.
[13] L.G. Zhang, Z.M. Xu, A critical review of material flow, recycling technologies, challenges and future strategy for scattered metals from minerals to wastes, J. Cleaner Prod., 202 (2018) 1001–1025.
[14] G.Q. Liu, Y.F. Wu, A.J. Tang, D. Pan, B. Li, Recovery of scattered and precious metals from copper anode slime by hydrometallurgy: a review, Hydrometallurgy, 197 (2020) 105460, doi: 10.1016/j.hydromet.2020.105460.
[15] J.W. Kim, A.S. Lee, S.G. Yu, J.W. Han, En masse pyrolysis of flexible printed circuit board wastes quantitatively yielding environmental resources, J. Hazard. Mater., 342 (2018) 51–57.
[16] L.L. Wang, Q. Li, Y. Li, X.Y. Sun, J.S. Li, J.Y. Shen, W.Q. Han, L.J. Wang, A novel approach for recovery of metals from waste printed circuit boards and simultaneous removal of iron from steel pickling waste liquor by two-step hydrometallurgical method, Waste Manage. (Oxford), 71 (2018) 411–419.
[17] J. Demol, E. Ho, G. Senanayake, Sulfuric acid baking and leaching of rare earth elements, thorium and phosphate from a monazite concentrate: effect of bake temperature from 200°C to 800°C, Hydrometallurgy, 179 (2018) 254–267.
[18] J.L. Su, X. Lin, S.L. Zheng, R. Ning, W.B. Lou, W. Jin, Mass transport-enhanced electrodeposition for the efficient recovery of copper and selenium from sulfuric acid solution, Sep. Purif. Rev., 182 (2017) 160–165.
[19] W.B. Lou, W.Q. Cai, P. Li, J.L. Su, S.L. Zheng, Y. Zhang, W. Jin, Additives-assisted electrodeposition of fine spherical copper powder from sulfuric acid solution, Powder Technol., 326 (2018) 84–88.
[20] M.D. Machado, E.V. Soares, H.M. Soares, Selective recovery of chromium, copper, nickel, and zinc from an acid solution using an environmentally friendly process, Environ. Sci. Pollut. Res. Int., 18 (2011) 1279–1285.
[21] C. Liu, T. Wu, P.C. Hsu, J. Xie, J. Zhao, K. Liu, J. Sun, J.W. Xu, J. Tang, Z.W. Ye, D.C. Lin, Y. Cui, Direct/alternating current

electrochemical method for removing and recovering heavy metal from water using graphene oxide electrode, ACS Nano, 13 (2019) 6431–6437.
[22] E. De Beni, W. Giurlani, L. Fabbri, R. Emanuele, S. Santini, C. Sarti, T. Martellini, E. Piciollo, A. Cincinelli, M. Innocenti, Graphene-based nanomaterials in the electroplating industry: a suitable choice for heavy metal removal from wastewater, Chemosphere, 292 (2022) 133448, doi: 10.1016/j.chemosphere.2021.133448.
[23] Y. Delgado, F.J. Fernandez-Morales, J. Llanos, An old technique with a promising future: recent advances in the use of electrodeposition for metal recovery, Molecules, 26 (2021) 5525, doi: 10.3390/molecules26185525.
[24] D.R. Turner, G.R. Johnson, The effect of some addition agents on the kinetics of copper electrodeposition from a sulfate solution, J. Electrochem. Soc., 190 (1962) 798–804.
[25] C.X. Ji, G. Oskam, P.C. Searson, Electrodeposition of copper on silicon from sulfate solution, J. Electrochem. Soc., 148 (2001) C746–C752.
[26] L.P. Wang, G.Q. Zhang, W.J. Guan, L. Zeng, Q. Zhou, Y. Xia, Q. Wang, Q.G. Li, Z.Y. Cao, Complete removal of trace vanadium from ammonium tungstate solutions by solvent extraction, Hydrometallurgy, 179 (2018) 268–273.
[27] D. Torres, L. Madriz, R. Vargas, B.R. Scharifker, Electrochemical formation of copper phosphide from aqueous solutions of Cu(II) and hypophosphite ions, Electrochim. Acta, 354 (2020) 136705, doi: 10.1016/j.electacta.2020.136705.
[28] T. Kekesi, M. Isshiki, Electrodeposition of copper from pure cupric chloride hydrochloric acid solutions, J. Electroanal. Chem., 27 (1997) 982–990.
[29] M.Y. Wang, X.Z. Gong, Z. Wang, Sustainable electrochemical recovery of high-purity Cu powders from multi-metal acid solution by a centrifuge electrode, J. Cleaner Prod., 204 (2018) 41–49.
[30] F.I. Lizama-Tzec, L. Canché-Canul, G. Oskam, Electrodeposition of copper into trenches from a citrate plating bath, Electrochim. Acta, 56 (2011) 9391–9396.
[31] R. Torres, G.T. Lapidus, Closed circuit recovery of copper, lead and iron from electronic waste with citrate solutions, Waste Manage. (Oxford), 60 (2017) 561–568.
[32] X.T. Yu, M.Y. Wang, X.Z. Gong, Z.C. Guo, Z. Wang, S.Q. Jiao, Self-supporting porous CoP-based films with phase-separation structure for ultrastable overall water electrolysis at large current density, Adv. Energy Mater., 34 (2018) 1802445, doi: 10.1002/aenm.201802445.
[33] B. Segura-Bailón, G.T. Lapidus, Selective recovery of copper contained in waste PCBs from cellphones with impurity inhibition in the citrate-phosphate system, Hydrometallurgy, 203 (2021) 105699, doi: 10.1016/j.hydromet.2021.105699.
[34] K. Suwannahong, J. Sripirom, C. Sirilamduan, V. Thathong, T. Kreetachart, P. Panmuang, A. Deepatana, S. Punbut, S. Wongcharee, H. Hamad, Selective chelating resin for copper removal and recovery in aqueous acidic solution generated from synthetic copper-citrate complexes from bioleaching of e-waste, Adsorpt. Sci. Technol., 2022 (2022) 1–14.
[35] S.S. Goh, M. Rafatullah, N. Ismail, M. Alam, M.R. Siddiqui, E.K. Seow, Separation of chromium(VI), copper and zinc: chemistry of transport of metal ions across supported liquid membrane, Membranes (Basel), 12 (2022) 685, doi: 10.3390/membranes12070685.
[36] J.E. Terrazas-Rodríguez, S. Gutiérrez-Granados, M.A. Alatorre-Ordaz, C. Ponce de León, F.C. Walsh, A comparison of the electrochemical recovery of palladium using a parallel flat plate flow-by reactor and a rotating cylinder electrode reactor, Electrochim. Acta, 56 (2011) 9357–9363.
[37] W. Jin, M.Q. Hu, J.G. Hu, Selective and efficient electrochemical recovery of dilute copper and tellurium from acidic chloride solutions, ACS Sustainable Chem. Eng., 6 (2018) 13378–13384.
[38] M.Q. Hu, Z. Sun, J.G. Hu, H. Lei, W. Jin, Simultaneous phenol detoxification and dilute metal recovery in cyclone electrochemical reactor, Ind. Eng. Chem. Res., 58 (2019) 12642–12649.
[39] E. Mostafa, S. Martens, L. Asen, J. Zečević, O. Schneider, C. Argirusis, The influence of the ultrasound characteristics on the electrodeposition of copper from chloride-based electrolytes, J. Electroanal. Chem., 892 (2021) 115318, doi: 10.1016/j.jelechem.2021.115318.
[40] W. Jin, P.I. Laforest, A. Luyima, W. Read, L. Navarro, M.S. Moats, Electrolytic recovery of bismuth and copper as a powder from acidic sulfate effluents using an emew® cell, RSC Adv., 5 (2015) 50372–50378.
[41] J.A. Barragan, C. Ponce de Leon, J.R. Aleman Castro, A. Peregrina-Lucano, F. Gomez-Zamudio, E.R. Larios-Duran, Copper and antimony recovery from electronic waste by hydrometallurgical and electrochemical techniques, ACS Omega, 5 (2020) 12355–12363.
[42] G. Maduraiveeran, J. Wei, Nanomaterials based electrochemical sensor and biosensor platforms for environmental applications, Trends Environ. Anal. Chem., 13 (2017) 10–23.
[43] S. Rode, C. Henninot, C. Vallières, M. Matlosz, Complexation chemistry in copper plating from citrate baths, J. Electrochem. Soc., 151 (2004) C405–C411.
[44] W. Shao, G. Pattanaik, G. Zangari, Influence of chloride anions on the mechanism of copper electrodeposition from acidic sulfate electrolytes, J. Electrochem. Soc., 154 (2007) D201–D207.